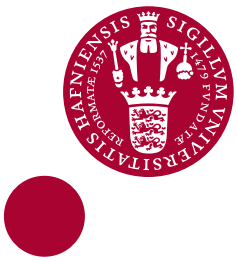

Cancer cells' ability to mechanically adjust to extracellular matrix stiffness correlates with their invasive potential

Wullkopf, Lena; West, Ann Katrine V.; Leijnse, Natascha; Cox, Thomas R.; Madsen, Chris D.; Oddershede, Lene B.; Erler, Janine T.

Published in:
Molecular Biology of the Cell

DOI:
10.1091/mbc.E18-05-0319

Publication date:
2018

Document version
Publisher's PDF, also known as Version of record

Cancer cells' ability to mechanically adjust to extracellular matrix stiffness correlates with their invasive potential

Lena Wullkopf[a,b], Ann-Katrine V. West[b], Natascha Leijnse[b], Thomas R. Cox[a,c], Chris D. Madsen[a,d], Lene B. Oddershede[b,*], and Janine T. Erler[a,*]

[a]Biotech Research and Innovation Centre (BRIC), University of Copenhagen, 2200 Copenhagen, Denmark; [b]Niels Bohr Institute, University of Copenhagen, 2100 Copenhagen, Denmark; [c]Garvan Institute of Medical Research and the Kinghorn Cancer Centre, Cancer Division, St Vincent's Clinical School, Faculty of Medicine, University of New South Wales, Sydney, NSW 2010, Australia; [d]Department of Laboratory Medicine, Division of Translational Cancer Research, Lund University, 223 81 Lund, Sweden

ABSTRACT **Increased tissue stiffness is a classic characteristic of solid tumors. One of the major contributing factors is increased density of collagen fibers in the extracellular matrix (ECM). Here, we investigate how cancer cells biomechanically interact with and respond to the stiffness of the ECM. Probing the adaptability of cancer cells to altered ECM stiffness using optical tweezers–based microrheology and deformability cytometry, we find that only malignant cancer cells have the ability to adjust to collagen matrices of different densities. Employing microrheology on the biologically relevant spheroid invasion assay, we can furthermore demonstrate that, even within a cluster of cells of similar origin, there are differences in the intracellular biomechanical properties dependent on the cells' invasive behavior. We reveal a consistent increase of viscosity in cancer cells leading the invasion into the collagen matrices in comparison with cancer cells following in the stalk or remaining in the center of the spheroid. We hypothesize that this differential viscoelasticity might facilitate spheroid tip invasion through a dense matrix. These findings highlight the importance of the biomechanical interplay between cells and their microenvironment for tumor progression.**

Monitoring Editor
Dennis Discher
University of Pennsylvania

Received: May 24, 2018
Revised: Jul 24, 2018
Accepted: Jul 31, 2018

INTRODUCTION

Metastatic spread is responsible for more than 90% of cancer-related deaths (Sporn, 1996). The progression from a primary tumor to a disseminated metastatic disease is a complex process. Cancer cells interact with their noncellular surroundings, the extracellular matrix (ECM), at each step of the metastatic process (Venning *et al.*, 2015). The expression and deposition of many ECM proteins is significantly altered during the progression of tumors, leading to both biochemical and biomechanical changes, including stiffness changes, of the tumor microenvironment. Altered ECM stiffness is a classic characteristic of tumors, used for diagnosis by palpation or magnetic resonance elastography for many decades. Studies have shown that breast cancer tissues exhibit an elastic modulus that is around 10-fold stiffer than normal mammary tissue (Levental *et al.*, 2009). Moreover, increased matrix stiffness is shown to drive a malignant transformation in the breast (Butcher *et al.*, 2009; Levental *et al.*, 2009).

One major contributing factor to altered ECM stiffness is increased deposition of type I collagen (Provenzano *et al.*, 2008a; Cox and Erler, 2011; Lu *et al.*, 2012). Fibrillar collagen I builds a physical scaffold providing tensile strength and stiffness to the tissue (Erler and Weaver, 2009). The density and alignment of collagen fibrils vary in different tissues and support distinct mechanical and biological functions of an organ. Hence, alteration of collagen deposition or posttranslational modifications and cross-linking observed in

This article was published online ahead of print in MBoC in Press (http://www.molbiolcell.org/cgi/doi/10.1091/mbc.E18-05-0319) on August 9, 2018.

The authors declare no competing interests.

Author contributions: L.W., T.R.C., C.D.M, L.B.O., and J.T.E. designed the experimental study. L.W., A.V.W., and N.L. performed the experiments. L.W., L.B.O., and J.T.E. wrote the paper. All authors approved the submitted version of the paper.

*Address correspondence to: Janine T. Erler (Janine.erler@bric.ku.dk) or Lene B. Oddershede (Oddershede@nbi.ku.dk).

Abbreviations used: 3D, three-dimensional; ECM, extracellular matrix; FAK, focal adhesion kinase; FAK 14, FAK inhibitor 14; FBS, fetal bovine serum; LatB, latrunculin B; RT-DC, real-time deformability cytometry.

pathological settings, such as fibrosis and cancer, vastly alter the physical properties of tissues and can contribute to disease manifestation and progression (Butcher *et al.*, 2009; Erler and Weaver, 2009; Cox and Erler, 2011; Pickup *et al.*, 2014).

It has long been known that the metastatic cascade is a physically demanding process. Cancer cells have to both resist and apply forces on the environment while invading the dense ECM. In addition, the ability to adapt to physical conditions is essential for metastatic colonization, as secondary tumor sites often exhibit vastly different conditions than the organ of tumor origin.

In this study, we focus on intracellular responses to collagen I density changes in the microenvironment and link them to the invasive status of the cancer cells. Although it is well established that an increased deposition and crosslinking of collagen I promotes the metastatic progression of tumors (Provenzano *et al.*, 2008b; Levental *et al.*, 2009; Conklin *et al.*, 2011), little is known of the intracellular mechanical changes, especially cytoplasmic viscoelasticity, in reaction to increased collagen density and how this relates to the invasive potential of the cells. To probe the cytoplasmic viscoelasticity, we use a tightly focused laser beam, an optical trap, capable of tracking the motility of endogenously occurring lipid granules inside living cells (Tolić-Nørrelykke *et al.*, 2004; Leijnse *et al.*, 2012) deeply embedded in collagen matrices of different densities. Performing these intracellular microrheology measurements in three-dimensional (3D) cultured single cancer cells and in cancer spheroids in matrices of different collagen I concentrations allows us to measure the intracellular mechanical response of cancer cells to extracellular stiffness dependent on their invasive status.

RESULTS AND DISCUSSION

Microrheological measurements inside cancer cells cultured in a 3D matrix

To quantify the intracellular viscoelasticity of cancer cells cultured in 3D matrices of varying stiffness, we monitored the thermal fluctuations of intracellular tracers in the form of endogenous lipid granules using an optical trap equipped with a photodiode detection system, as sketched in Figure 1A.

The position of an optically trapped lipid granule in the viscoelastic cytoplasm of living cells is denoted $x(t)$, t being time. The dynamics of the trapped granule can be described by a modified Langevin equation (Tolić-Nørrelykke *et al.*, 2004). The Langevin equation can be Fourier transformed to yield the positional power spectrum, $Px(f) \equiv \left\langle \left|\tilde{x}(f)\right|^2 \right\rangle$, where $\tilde{x}(f)$ denotes the Fourier transform of $x(t)$ and f is frequency. For frequencies larger than the corner frequency, f_c (defined in *Materials and Methods*), the power spectrum, $P_x(f)$, scales with an exponent, α:

$$P_x(f) \propto \frac{1}{f^{(1+\alpha)}} \qquad (1)$$

This scaling exponent, α, carries information about the local viscoelastic landscape (Tolić-Nørrelykke *et al.*, 2004; Selhuber-Unkel *et al.*, 2009). Subdiffusion of the tracer is characterized by $\alpha < 1$, normal Brownian motion by $\alpha = 1$, and superdiffusion by $\alpha > 1$. In a cell, cytoplasmic subdiffusion is the dominating mode of diffusion (Tolić-Nørrelykke *et al.*, 2004). In this regime, the environment possesses viscoelastic properties: the closer α is to 1, the more viscous the local environment; the closer α is to 0, the more elastic the environment. Hence, differences in the scaling exponent of a tracer in the cytoplasm may reflect the degree of molecular crowding and, therefore, changes in the abundance or assembly of macromolecular complexes such as the components of the cytoskeleton (Figure 1B). The influence of molecular crowding on diffusion was previously shown in heterochromatin-rich regions of the nucleus (Bancaud *et al.*, 2009). Despite areas particularly rich in DNA, RNA and proteins show only a moderate hindrance for fluorescent tracers, and they could detect a slower diffusion of the tracers in these regions.

The positional time series of a trapped lipid granule was Fourier transformed, and the power spectrum was calculated using Matlab (Hansen *et al.*, 2006; Selhuber-Unkel *et al.*, 2009). The power spectrum was fitted at frequencies above the corner frequencies using Eq. 1, while taking into account the filtering effect of the photodiode (Berg-Sørensen *et al.*, 2003), thus yielding the scaling exponent, α (see *Materials and Methods*).

Invasive cancer cells adjust their intracellular and overall viscoelasticity to ECM density

We investigated the microrheological properties of cancer cell pairs of different invasive potential: the breast cancer cell lines 4T1 and 67NR as well as MDA-MB-231 and MCF7; colorectal cancer lines SW620 and SW480; and the pancreatic cancer cell lines $KP^{R172H}C$ and $KP^{fl}C$ (Figure 1C). We changed the mechanical properties of the cells' microenvironment by culturing the cancer cells in 3D collagen matrices of various collagen concentrations. We quantified the stiffness of the matrices by shear rheology. For the collagen I matrix of 1 mg/ml, a mean Young's modulus of $Y = 377 \pm 68$ Pa was obtained. This value corresponds well to values of healthy soft tissues such as the lung or mammary gland (Cox and Erler, 2011). The high collagen I concentration, 4 mg/ml collagen I, had a Young's modulus of $Y = 1199 \pm 218$ Pa (Figure 1D). Representative images of the different cancer cell lines after 24 h in the different matrices are shown in Figure 1E and Supplemental Figure S1. Increasing the collagen concentration increases both matrix density and stiffness (Figure 1, D and E, and Supplemental Figure S1), producing a state that resembles tissue stiffening of a primary tumor site, as has been shown to be occur during cancer progression of the mammary gland (Erler and Weaver, 2009; Levental *et al.*, 2009), and other stiffer tissue types, such as the liver, that are sites for colonization of metastasis (Yeh *et al.*, 2002).

All cancer cells showed viscoelastic properties with scaling exponents in the interval of $\alpha = 0.53$–0.64 when cultured within 3D matrices. However, there was a striking difference in the ability to adjust to the environment between malignant and benign cell lines: noninvasive cell lines did not show significant changes in α when cultured in collagen gels of different concentrations. In contrast, all invasive cell lines showed strong intracellular adjustments when cultured within different collagen I matrices (Figure 1, F–I, and Table 1).

The MDA-MB-231 and $KP^{R172H}C$ cell lines, which displayed a highly viscous cytoplasm (as characterized by a relatively high α) in 1 mg/ml collagen I matrices, became more elastic when seeded in matrices of higher collagen concentrations, as quantified by the scaling exponent decreasing from $\alpha = 0.64 \pm 0.09$ to $\alpha = 0.61 \pm 0.09$ and from $\alpha = 0.63 \pm 0.11$ to $\alpha = 0.55 \pm 0.11$, respectively (Figure 1, F and G, and Table 1). For the invasive 4T1 and SW620 cells, which were more elastic in soft matrices, we observed the opposite response: an increase in viscosity as a response to matrix density (Figure 1, H and I).

To probe whether the elasticity of the entire cell is adjusted in a manner consistent with the observed changes in the local cytoplasmic viscoelasticity, we performed real-time deformability cytometry (RT-DC) of the cancer cells. RT-DC is a high-throughput technique that probes the deformation of cells in a microfluidic channel (Figure 2A), allowing an extraction of the cellular apparent Young's

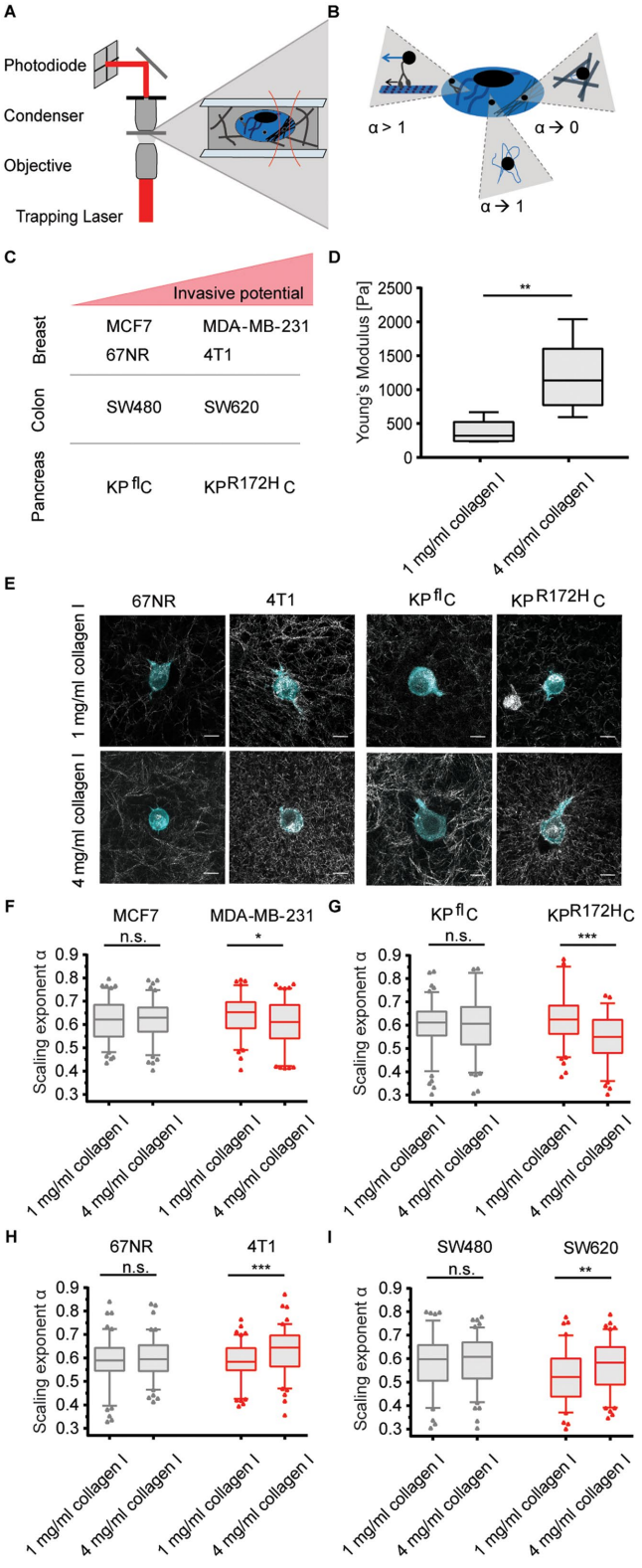

FIGURE 1: The ability to adjust cytoplasmic viscoelasticity to mechanical properties of the environment correlates with cancer cell invasiveness. (A) Illustration of the optical trapping setup. (B) Schematic illustration of possible origins of different α values: α→1 describes tracer movement in a purely viscous environment; α→0 describes confined tracer motion, e.g., in a densely packed, more elastic cytoplasm; α > 1 indicates superdiffusion, possibly mediated by active motor transportation of a granule along microtubuli. (C) Overview of the cancer cell pairs used in the microrheological measurements. (D) Young's moduli of 1 and 4 mg/ml collagen I matrices determined by shear rheology. (E) Representative confocal images of mEmerald-lifeAct-7–labeled 4T1 and 67NR breast cancer and $KP^{R172H}C$ and $KP^{fl}C$ pancreatic cancer cells cultured in matrices of 1 or 4 mg/ml rat-tail collagen I. Scale bars: 10 µm. (F) Scaling exponents, α, characterizing the intracellular lipid granule diffusion in human breast cancer cell lines MDA-MB-231 and MCF7 at different matrix stiffnesses. The noninvasive cell line (MCF7) is depicted in gray, the highly invasive (MDA-MB-231) in red. (G) Same as F, but for pancreatic cancer cell lines $KP^{R172H}C$ (red, invasive) and $KP^{fl}C$ (gray, noninvasive). (H) Same as F, but for mouse breast cancer cell lines 4T1 (red, invasive) and 67NR (gray, noninvasive). (I) Same as F, but for colorectal cancer cell lines SW620 (red, invasive) and SW480 (gray, noninvasive). Box plot of 5th to 95th percentile. ***, $p < 0.001$; **, $p < 0.01$; *, $p < 0.05$; n.s., not significant in a Mann-Whitney test (two-tailed).

modulus (Otto *et al.*, 2015; Mokbel *et al.*, 2017). Recently, it has been used to monitor physical changes of the malignant transformation of blood cells (Toepfner *et al.*, 2018); however, it has not been combined with soft cell culture to date.

After 24 h of culture on matrices of various concentrations of collagen I, only the invasive cancer cells suggested differences in their deformation (Supplemental Figure S2) and cellular elasticity (Figure 2) dependent on their previous culture conditions. By contrast, noninvasive cancer cell lines showed a constant overall elasticity.

Although the large variability of the measurements comes at the expense of statistical significance, RT-DC suggests similar mechanical changes within the invasive cell lines, with the MDA-MB-231 and $KP^{R172H}C$ expressing a more elastic phenotype when exposed to dense collagen networks, while the 4T1 breast cancer cell line suggests the opposite response. The invasive colorectal cancer cell line SW620, however, showed no differential elasticity on different matrices (Figure 2E).

The microrheology and RT-DC data therefore indicate that there is no apparent simple rule of intracellular adjustments of the cellular biomechanics, yet only malignant cells are able to adapt their viscoelasticity to the environment. The mechanical adjustments of MDA-MB-231 cells were recently confirmed by a study by Kim *et al.* (2018). Although the authors used particle-tracking microscopy, a method of limited temporal and spatial resolution, they were able to confirm intracellular stiffening in response to higher collagen concentrations.

Previous studies of the intracellular creep compliance of 3D cultured prostate cancer cells (Baker *et al.*, 2009) and mammary epithelial cells (MECs) (Baker *et al.*, 2010) revealed solely intracellular mechanical adjustments in transformed cells, but not in normal epithelial cells. As in our study, different cell types showed opposite adjustments to ECM stiffness with the prostate cells becoming softer and the transformed MECs stiffer in matrices of higher collagen concentration. However, these studies did merely focus on cell transformation, not on different cancer cell stages and invasive potential, and they have the limitation of probing only the endocytotic pathway, as the authors use endocytosed beads as microrheology tracers.

Nevertheless, we are aware that the chosen 3D collagen culture system has limitations as well. Increasing collagen concentration does alter matrix stiffness, pore size, and the abundance of integrin ligands simultaneously (Provenzano *et al.*, 2009; Miron-Mendoza *et al.*, 2010; Ulrich *et al.*, 2010; Antoine *et al.*, 2014; Cassereau *et al.*, 2015). Hence, all intracellular changes observed in this study cannot be solely attributed as mechanically mediated but could be a combined response to biochemical and biophysical stimuli.

To avoid this mixed influence, many previous publications used polyacrylamide gels of varying stiffness coated with the same

	Invasive		Noninvasive	
	1 mg/ml collagen I	4 mg/ml collagen I	1 mg/ml collagen I	4 mg/ml collagen I
MDA-MB-231	0.64 ± 0.09	0.61 ± 0.09		
MCF7			0.63 ± 0.09	0.62 ± 0.08
$KP^{R172H}C$	0.63 ± 0.11	0.55 ± 0.11		
$KP^{fl}C$			0.61 ± 0.09	0.60 ± 0.12
4T1	0.59 ± 0.08	0.63 ± 0.09		
67NR			0.59 ± 0.09	0.60 ± 0.08
SW620	0.53 ± 0.11	0.57 ± 0.10		
SW480			0.58 ± 0.11	0.59 ± 0.10

Data are shown as mean ± SD, $n = 100$.

TABLE 1: Overview of the scaling exponents characterizing the viscoelasticity of the cancer cells' cytoplasm when cultured within 3D collagen matrices of varying stiffness.

amount of ECM protein. While this is a good way around changing ligand densities, it does not allow measurement of live cells in a 3D matrix, as the precursor components of the cells are highly toxic (Caliari and Burdick, 2016). In addition, it has been previously demonstrated that, while cells show a strong phenotypic response to increasing collagen concentrations when cultured on stiff matrices, one can see only a minor influence of collagen density on cell spreading in "soft cell cultures" that is comparable to our stiffness range (Engler *et al.*, 2004).

Cancer cell viscosity increases during invasion into 3D matrices

To investigate mechanical changes during the invasion of cancer cells, we performed microrheology on a 3D spheroid invasion assay. Thermal fluctuations of lipid granules in cells remaining in the center of the spheroid, at the tip, and in the stalk of invading branches were examined (Figure 3A). This experimental setup allows a comparison of the intracellular viscoelasticity of cells of the same origin during the process of invasion.

Both the highly invasive pancreatic cancer cell line $KP^{R172H}C$ and breast cancer cell line 4T1 showed significant mechanical adjustments during the invasive process. In both matrices, cells located at the tips of the invading branches exhibited significantly higher scaling exponents than cells remaining in the centers of the spheroids. In collagen matrices of 1 mg/ml, 4T1 cells at the tip of an invading branch showed a mean scaling exponent of $\alpha = 0.60 \pm 0.09$ in comparison to $\alpha = 0.56 \pm 0.08$ of cells in the center ($p = 0.043$) (Figure 3B and Supplemental Table S1). $KP^{R172H}C$ cells at the invasive tip showed a mean scaling exponent of $\alpha = 0.62 \pm 0.09$. The cells in the stalk had $\alpha = 0.61 \pm 0.08$, and cells remaining in the center of the sphere had $\alpha = 0.59 \pm 0.10$ (comparison of the viscoelasticity of cells at the tip to cells in the center: $p = 0.0425$) (Figure 3C and Supplemental Table S1). Notably, consistent with the results displayed in Figure 1, G and H, 4T1 cells in all positions within the sphere became more viscous when the sphere was seeded in the high-density matrix, while the $KP^{R172H}C$ cell line showed an overall reduction in viscoelasticity when seeded in a stiffer matrix.

To probe whether matrix stiffness or cellular status is dominant in determining intracellular mechanics, we also probed the intracellular viscoelasticity in the spheroid invasion system of cells of noninvasive status, the 67NR and $KP^{fl}C$ cells, cultured in collagen gels of 1 and 4 mg/ml. Generally, these cell lines invaded poorly into the collagen gels. Consistent with reports showing cell stiffness driving more aggressive cell behavior, the 67NR showed a more invasive phenotype in the collagen gels of higher concentration and stiffness (Paszek *et al.*, 2005; Baker *et al.*, 2013). Regarding the intracellular viscoelasticity in the cancer cell lines of noninvasive status, we overall observed the same trends for the cells as for their invasive counterparts, with the cells at the tips of invasive branches exhibiting a more viscous cytoplasm than cells in the centers of the spheroids (Supplemental Figure S3). However, the differential increase in viscosity of the cells invading into the gels was significant only for the 67NR cells in matrices of 4 mg/ml collagen I. Hence, the data suggest a context-dependent influence of matrix properties on intracellular mechanics that, in the case of the 67NR line, can be dominant over the noninvasive status of the cells.

To demonstrate the sensitivity of the setup to mechanical changes in the cell (e.g., due to changes in the cytoskeleton), we short-term treated spheroids that had invaded the collagen matrices with latrunculin B (LatB), a toxin that disrupts actin microfilaments (El Sayed *et al.*, 2006). Cancer cells incubated with LatB obtained a round phenotype accompanied by an increase in intracellular viscosity in cells at all positions within the spheroid (Supplemental Figure S4, A and B, and Supplemental Table S1).

As extracellular stiffness has been shown to induce focal adhesion kinase (FAK) activation (Schedin and Keely, 2011; Bae *et al.*, 2014), we investigated the role of FAK in the adjustments of the mechanical status of the cancer cells during the invasive process. FAK inhibitor 14 (FAK 14) was able to reduce the levels of phosphorylated FAK in a concentration-dependent manner (Supplemental Figure S4, C and D) and blocked invasion of both the 4T1 breast and $KP^{R172H}C$ pancreatic cancer cell lines (Supplemental Figure S4, E and F). In the microrheology experiments, $KP^{R172H}C$ and 4T1 spheroids were allowed to invade collagen matrices for ~2.5 d before they were treated with FAK 14. Inhibiting FAK signaling made the cancer cells insensitive to changes in the microenvironment and diminished any differential viscoelasticity dependent on the position of the cells within the spheroid. For 4T1 cells, the scaling exponent leveled out at $\alpha \sim 0.60$. $KP^{R172H}C$ cells plateaued at $\alpha \sim 0.61$ (Supplemental Figure S4, G and H, and Supplemental Table S1). These findings support that FAK is instrumental for the observed intracellular biomechanical adaptations of invading cancer cells.

How cancer cells change mechanically during the progression of the disease is highly debated. Increased viscosity allows migration through small pores (Wolf *et al.*, 2003; Guck *et al.*, 2005; Swaminathan *et al.*, 2011). However, higher elasticity is associated with a stronger cytoskeleton and may be linked to higher force generation, which was also shown to correlate with cancer cell

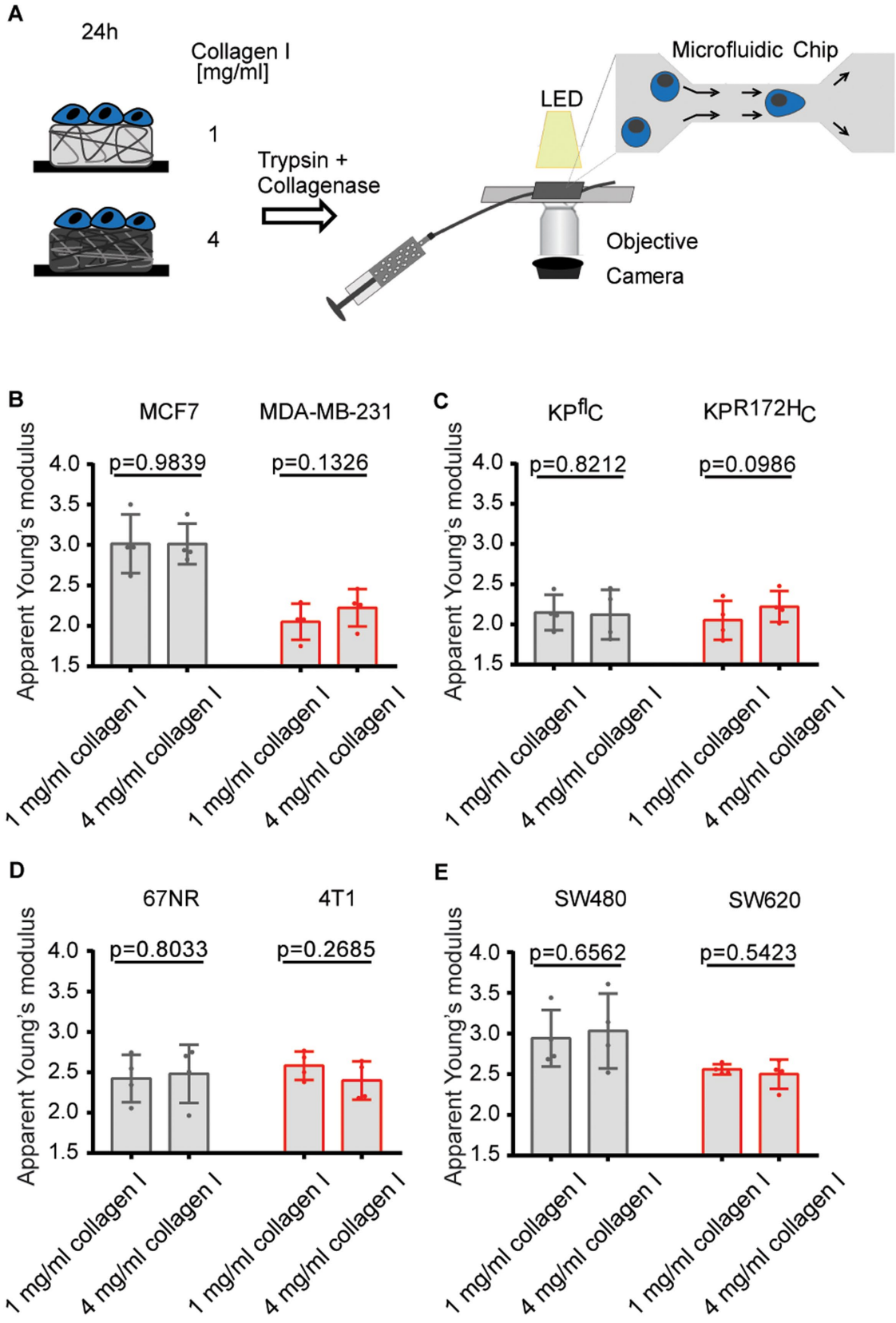

FIGURE 2: The ability to adjust cellular elasticity to mechanical properties of the environment correlates with cancer cell invasiveness. (A) Schematic of RT-DC of cancer cells cultured on matrices of different collagen I concentration. After detachment, suspended cells experience high shear forces when entering a 20-μm channel. The resulting deformation is imaged by a high-speed camera. (B–E) Overview of the median apparent Young's moduli of pairs of human breast cancer (B), pancreatic cancer (C), mouse breast cancer (D), and colorectal cancer (E) cell lines after 24-h culture on different collagen I matrices. Error bars denote 1 SD, $n = 4$. p Values are derived from a paired Student's t test.

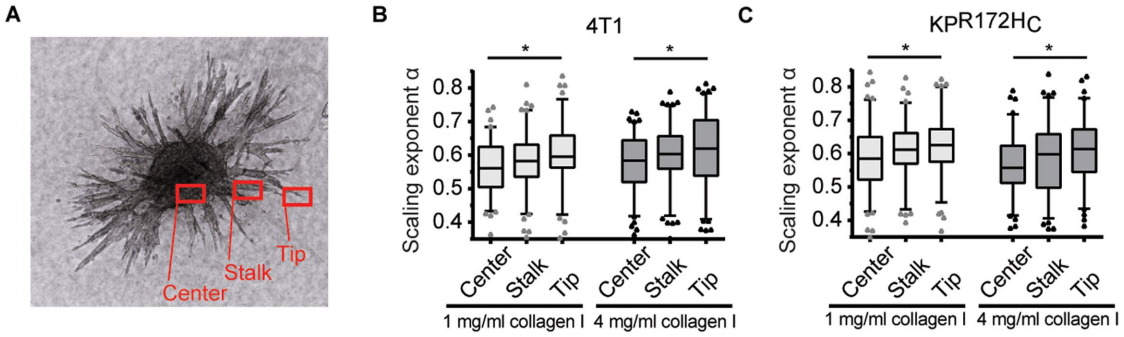

FIGURE 3: Cancer cells show a differential increase in viscosity during the process of 3D invasion. (A) Image of a 4T1 spheroid 72 h after being embedded within a matrix of 4 mg/ml collagen I. The different regions ("Center," "Stalk," and "Tip") are indicated in red. (B, C) Assessment of the scaling exponent, α, characterizing intracellular lipid granule diffusion in 4T1 (B) and $KP^{R172H}C$ (C) in the center, in the stalk, or at the tip of an invading branch of a spheroid embedded in matrices of 1 or 4 mg/ml collagen I. *, $p < 0.05$ in an ordinary one-way analysis of variance followed by a Holm-Sidak's multiple-comparisons test.

invasion (Solon *et al.*, 2007; Koch *et al.*, 2012; Mekhdjian *et al.*, 2017). Performing microrheology in an assay highly relevant to biology, in which a cancer spheroid is embedded in and invades a three-dimensional matrix, allows an elegant comparison of cells of the same origin exhibiting different migratory behavior during the measurement phase. Here, we detected that, for both the 4T1 and $KP^{R172H}C$ cell lines, cells located at the tips of the invasive strands of the spheroid are significantly more viscous than those located in the spheroid center. This consistent increase in intracellular viscosity during the actual process of invasion supports the hypothesis that an increased compliance allows the cells to squeeze through a confined environment (Wolf *et al.*, 2003; Guck *et al.*, 2005). However, we cannot resolve whether cells at the tips became more viscous during the process of invasion or whether the cells with the highest invasive capacity exhibit the most viscous cytoplasm. Overall, the biomechanical adjustments during invasion do not overrule the distinctive mechanical state of the cancer cells when cultured in matrices of different stiffness. In both the 4T1 and $KP^{R172H}C$ cells, we were still able to detect differences in their overall viscoelasticity in response to diverse microenvironments.

ECM stiffness and density translates to changes of cellular signaling and phenotype by a multistep process. Cells are reported to feel the rigidity of their environment by pulling against the ECM, involving components of the force-sensing machinery and cytoskeleton (Schedin and Keely, 2011). By targeting FAK in the microrheology experiments during cancer sphere invasion, we can prove the overlap of signaling components involved in force and environment sensing of invasive cancer cells. Inhibiting actin polymerization or FAK signaling not only made the cancer cells insensitive to stiffness in their surroundings but also leveled out any differential mechanical status dependent on the positions of the cells within the spheroid. Interestingly, FAK-inhibited cancer cells showed an increased viscosity, which was also reported in a previous study (Mierke *et al.*, 2017). Nevertheless, FAK treatment inhibited invasion very efficiently, suggesting a different underlying biology for the intracellular changes during invasion.

Taken together, our studies combined 3D cultures with state-of-the-art biophysical tools, allowing us to study mechanical changes of cancer cells dependent on not only cancer progression but also the microenvironment. Different mechanical cues have been shown to either drive (Levental *et al.*, 2009) or block (Ricca *et al.*, 2018) cancer progression. However, the link to intracellular mechanical changes has been missing to date. We reveal a correlation between invasive potential and cancer cells' ability to mechanically adjust to the surrounding matrix. We hypothesize that this differential ability to adjust to matrix stiffness might aid colonization at physically different secondary sites in the body. Also, we report a consistent increase of cancer cell viscosity during the invasion in a three-dimensional invasion assay, demonstrating that, even within a cluster of cells of similar origin, there are differences in their viscoelastic properties dependent on their invasive behavior. Our results show that the distinctive mechanical state of the cells in the diverse microenvironments is also maintained in a cell cluster and is dependent on FAK signaling. Insight into these mechanisms may pave the way for novel drugs prohibiting biomechanical adjustments of cancer cells in response to changes in the tumor microenvironment.

MATERIALS AND METHODS

Cell culture

The 4T1 and 67NR breast cancer cell lines were a kind gift from Fred Miller (Wayne State University). The $KP^{R172H}C$ and $KP^{fl}C$ pancreatic cancer cell lines were a kind gift from Jennifer Morton (Beatson Institute). All other cell lines were purchased from the American Type Culture Collection. All cell lines were cultured at 37°C and 5% CO_2 and routinely tested negative for mycoplasma. The MCF7 cell line was cultured in DMEM/F-12 supplemented with 10% fetal bovine serum (FBS) and 1% penicillin/streptomycin (P/S). All other cell lines were cultured in DMEM containing GlutaMAX, 10% FBS, and 1% P/S.

Culturing cells on collagen I gels

Collagen mixtures of 1 or 4 mg/ml were prepared by mixing high concentration acid-extracted and cross-linked rat tail collagen I, sterile phosphate-buffered saline (PBS), and 5X collagen buffer containing 0.1M HEPES, 2% $NaHCO_3$, and α-MEM. The gels were allowed to polymerize at 37°C for 1 h before they were washed with PBS. Cells (3×10^5) were added and incubated for 24 h before RT-DC.

Three-dimensional collagen I cell culture

Cells were suspended in the collagen mixtures prepared as described earlier. After polymerization, the gels were washed once and incubated with normal culture medium for 24 h.

Cell transfections

The different cancer cell lines were transfected with mEmerald-lifeAct-7 (a kind gift from the Ivaska lab, Turku Centre for Biotechnology) using Lipofectamine 2000 and incubated for ~12 h before being embedded in 3D collagen matrices as described earlier.

Spheroid invasion assay

Cancer cell spheroids of 2×10^4 4T1 or $KP^{R172H}C$ cells were generated by the hanging drop technique (Chang *et al.*, 2017). The next day, the spheroids were embedded in collagen I matrices as described earlier. The spheroids were allowed to invade the collagen gels for 72 h before optical tweezers (OT) measurements. Treatments with FAK 14 (20 μM) or LatB (1 μM) were performed 24 h or 1–2 h before measurement, respectively. For the initial testing of FAK 14 (Supplemental Figure S4), the spheres were treated for 72 h.

Intracellular microrheology

Optical trapping of intracellular lipid granules in 3D cultured cells or cancer cell spheroids was performed using an optical tweezers setup equipped with a highly focused laser and a photodiode detection system implemented into an inverted Leica DMIRBE microscope. The laser beam (Nd:YVO4, 5W Spectra Physics BL106C, λ = 1064 nm, TEM∞) was tightly focused by a water-immersion objective (Leica, HCX PL APO 63×/1.2 NA). The trapping laser light was collected by a condenser (Leica, P1 1.40 oil S1) located in the back-focal plane and focused onto a quadrant photodiode (S5981; Hamamatsu). Data were acquired by an acquisition card (NI PCI-6040E) at a sampling frequency of 22 kHz and processed by custom-made LabVIEW programs (LabVIEW 2010; National Instruments). For the distances traveled by a trapped granule, the voltage output from the photodiode is linearly related to particle displacement with respect to the laser focus (Ott *et al.*, 2014). The positional time series, $x(t)$, was analyzed using Matlab (MathWorks) (Hansen *et al.*, 2006; Selhuber-Unkel *et al.*, 2009). From $x(t)$, we calculated the positional power spectrum, $Px(f) \equiv \left\langle \left| \tilde{x}(f) \right|^2 \right\rangle$. The dynamics of a trapped lipid granule is well described by a modified Langevin equation. The corner frequency of the power spectrum of the Fourier-transformed modified Langevin equation, f_c, is defined as $f_c = \kappa / 2\pi\gamma$, where κ is the spring constant characterizing the harmonic potential of the optical trap and γ is the friction coefficient of a lipid granule. f_c denotes the frequency below which the granule feels the restoring potential of the optical trap (Tolić-Nørrelykke *et al.*, 2004). For frequencies larger than f_c, the power spectrum, $P_x(f)$, scales with an exponent, α (see Eq. 1). The[frequency interval used for fitting Eq. 1 to the data was 500–9900 Hz, allowing the extraction of the scaling exponent α.

Confocal imaging

LifeAct-7–transfected cancer cells cultured in 3D collagen matrices were imaged on an inverted Leica SP5 confocal microscope with a 63× water objective (Leica, HC PL APO 63×/1.20). mEmerald-life-Act-7 was excited at 488 nm, and the collagen fibers were imaged using the 633-nm laser in fluorescence mode without enhanced dynamics.

RT-DC

Cancer cells cultured on collagen I matrices were trypsinized for 20 min; this was followed by collagenase treatment (4 mM collagenase II and IV) for 10 min at 37°C. The enzymatic reaction was stopped using DMEM containing 20% FBS. Cell solutions were washed in PBS and resuspended in a final volume of 600 μl cell carrier buffer. The samples were analyzed in a cytometer (AcCellerator; Zellmechanik Dresden). The deformation, D, of the cells in a microfluidic chip with a constricted channel of 20 μm was recorded at a flow rate of 0.12 μl/s. The deformation is defined as $D = 1 - C$, where C is the circularity. The circularity is defined as $C = 2\sqrt{\pi A}/l$, where A is the projected cell area and l is its perimeter. The data were analyzed using the analysis software ShapeOut, version 0.8.4. The following filters were applied: range area, 50–400 μm; range area ratio, 1–1.05. The apparent Young's modulus Y of the cells was extracted from the filtered deformation data (Mietke *et al.*, 2015; Mokbel *et al.*, 2017).

Shear rheology

Relative stiffness of collagen I matrices were measured by shear rheology using a DHR-2–controlled strain rotational rheometer (TA Instruments) (Madsen *et al.*, 2015; Cox and Madsen, 2017). Collagen I gels of different concentrations were prepared 24 h before measurements as described earlier. Disks of 8-mm diameter were excised using a biopsy punch. Measurements were performed using an 8-mm sand-blasted parallel-plate geometry, a fixed frequency of 1 Hz, and an increasing strain from 0.2 to 1.2%. Storage moduli (G') at 0.3% strain were extracted, and the Young's moduli Y were determined the following relation: $Y = 2 \times G' (1 + \upsilon)$, where $\upsilon = 0.5$ for hydrogels (Cox and Madsen, 2017).

Immunoblotting

Inhibition of phosphorylation of FAK Tyr-397 was investigated by immunoblot. Cancer cells were incubated with 0, 3, 10, or 20 μM FAK 14 for 16 h before cell lysis, followed by standard immunoblotting using anti-FAK (phospho-Tyr-397) and anti–β-tubulin antibodies.

Statistics

All statistical tests were performed using GraphPad Prism. Normal distribution was tested in a D'Agostino and Pearson normality test, followed by the appropriate parametric or nonparametric test, as indicated in the figure legends (*, $p < 0.05$; **, $p < 0.01$; ***, $p < 0.001$; n.s.: not significant).

ACKNOWLEDGMENTS

We acknowledge financial support from Danish Research Council grant DFF-4002-00099, Danish National Research Foundation grant DNRF116, a Novo Nordisk Foundation Hallas Møller stipend, the National Health and Medical Research Council (NHMRC) of Australia, and the Ragnar Söderberg Foundation, Sweden.

REFERENCES

Antoine EE, Vlachos PP, Rylander MN (2014). Review of collagen I hydrogels for bioengineered tissue microenvironments: characterization of mechanics, structure, and transport. Tissue Eng Part B Rev 20, 683–696.

Bae YH, Mui KL, Hsu BY, Liu S-L, Cretu A, Razinia Z, Xu T, Puré E, Assoian RK (2014). A FAK-Cas-Rac-lamellipodin signaling module transduces extracellular matrix stiffness into mechanosensitive cell cycling. Sci Signal 7, ra57.

Baker AM, Bird D, Lang G, Cox TR, Erler JT (2013). Lysyl oxidase enzymatic function increases stiffness to drive colorectal cancer progression through FAK. Oncogene 32, 1863–1868.

Baker EL, Bonnecaze RT, Zaman MH (2009). Extracellular matrix stiffness and architecture govern intracellular rheology in cancer. Biophys J 97, 1013–1021.

Baker EL, Lu J, Yu D, Bonnecaze RT, Zaman MH (2010). Cancer cell stiffness: integrated roles of three-dimensional matrix stiffness and transforming potential. Biophys J 99, 2048–2057.

Bancaud A, Huet S, Daigle N, Mozziconacci J, Beaudouin J, Ellenberg J (2009). Molecular crowding affects diffusion and binding of nuclear proteins in heterochromatin and reveals the fractal organization of chromatin. EMBO J 28, 3785–3798.

Berg-Sørensen K, Oddershede L, Florin E-L, Flyvbjerg H (2003). Unintended filtering in a typical photodiode detection system for optical tweezers. J Appl Phys 93, 3167–3176.

Butcher DT, Alliston T, Weaver VM (2009). A tense situation: forcing tumour progression. Nat Rev Cancer 9, 108–122.

Caliari SR, Burdick JA (2016). A practical guide to hydrogels for cell culture. Nat Methods 13, 405–414.

Cassereau L, Miroshnikova YA, Ou G, Lakins J, Weaver VM (2015). A 3D tension bioreactor platform to study the interplay between ECM stiffness and tumor phenotype. J Biotechnol 193, 66–69.
Chang J, Lucas MC, Leonte LE, Garcia-Montolio M, Singh LB, Findlay AD, Deodhar M, Foot JS, Jarolimek W, Timpson P, *et al.* (2017). Preclinical evaluation of small molecule LOXL2 inhibitors in breast cancer. Oncotarget 8, 26066–26078.
Conklin MW, Eickhoff JC, Riching KM, Pehlke CA, Eliceiri KW, Provenzano PP, Friedl A, Keely PJ (2011). Aligned collagen is a prognostic signature for survival in human breast carcinoma. Am J Pathol 178, 1221–1232.
Cox T, Madsen C (2017). Relative stiffness measurements of cell-embedded hydrogels by shear rheology in vitro. Bio Protoc 7, DOI: 10.21769/BioProtoc.2101.
Cox TR, Erler JT (2011). Remodeling and homeostasis of the extracellular matrix: implications for fibrotic diseases and cancer. Dis Model Mech 4, 165–178.
El Sayed KA, Youssef DTA, Marchetti D (2006). Bioactive natural and semisynthetic latrunculins. J Nat Prod 69, 219–223.
Engler A, Bacakova L, Newman C, Hategan A, Griffin M, Discher D (2004). Substrate compliance versus ligand density in cell on gel responses. Biophys J 86, 617–628.
Erler JT, Weaver VM (2009). Three-dimensional context regulation of metastasis. Clin Exp Metastasis 26, 35–49.
Guck J, Schinkinger S, Lincoln B, Wottawah F, Ebert S, Romeyke M, Lenz D, Erickson HM, Ananthakrishnan R, Mitchell D, *et al.* (2005). Optical deformability as an inherent cell marker for testing malignant transformation and metastatic competence. Biophys J 88, 3689–3698.
Hansen PM, Tolić-Nørrelykke IM, Flyvbjerg H, Berg-Sørensen K (2006). tweezercalib 2.0: faster version of MatLab package for precise calibration of optical tweezers. Comput Phys Commun 174, 518–520.
Kim JE, Reynolds DS, Zaman MH, Mak M (2018). Characterization of the mechanical properties of cancer cells in 3D matrices in response to collagen concentration and cytoskeletal inhibitors. Integr Biol (Camb) 10, 232–241.
Koch TM, Münster S, Bonakdar N, Butler JP, Fabry B (2012). 3D traction forces in cancer cell invasion. PLoS One 7, e33476.
Leijnse N, Jeon JH, Loft S, Metzler R, Oddershede LB (2012). Diffusion inside living human cells. Eur Phys J Spec Top 204, 75–84.
Levental KR, Yu H, Kass L, Lakins JN, Egeblad M, Erler JT, Fong SF, Csiszar K, Giaccia A, Weninger W, *et al.* (2009). Matrix crosslinking forces tumor progression by enhancing integrin signaling. Cell 139, 891–906.
Lu P, Weaver VM, Werb Z (2012). The extracellular matrix: a dynamic niche in cancer progression. J Cell Biol 196, 395–406.
Madsen CD, Pedersen JT, Venning FA, Singh LB, Moeendarbary E, Charras G, Cox TR, Sahai E, Erler JT (2015). Hypoxia and loss of PHD2 inactivate stromal fibroblasts to decrease tumour stiffness and metastasis. EMBO Rep 16, 1394–1408.
Mekhdjian AH, Kai F, Rubashkin MG, Prahl LS, Przybyla LM, McGregor AL, Bell ES, Barnes JM, DuFort CC, Ou G, *et al.* (2017). Integrin-mediated traction force enhances paxillin molecular associations and adhesion dynamics that increase the invasiveness of tumor cells into a three-dimensional extracellular matrix. Mol Biol Cell 28, 1467–1488.
Mierke CT, Fischer T, Puder S, Kunschmann T, Soetje B, Ziegler WH (2017). Focal adhesion kinase activity is required for actomyosin contractility-based invasion of cells into dense 3D matrices. Sci Rep 7, 42780.
Mietke A, Otto O, Girardo S, Rosendahl P, Taubenberger A, Golfier S, Ulbricht E, Aland S, Guck J, Fischer-Friedrich E (2015). Extracting cell stiffness from real-time deformability cytometry: theory and experiment. Biophys J 109, 2023–2036.
Miron-Mendoza M, Seemann J, Grinnell F (2010). The differential regulation of cell motile activity through matrix stiffness and porosity in three dimensional collagen matrices. Biomaterials 31, 6425–6435.
Mokbel M, Mokbel D, Mietke A, Träber N, Girardo S, Otto O, Guck J, Aland S (2017). Numerical simulation of real-time deformability cytometry to extract cell mechanical properties. ACS Biomater Sci Eng 3, 2962–2973.
Ott D, Reihani SNS, Oddershede LB (2014). Crosstalk elimination in the detection of dual-beam optical tweezers by spatial filtering. Rev Sci Instrum 85, 053108.
Otto O, Rosendahl P, Mietke A, Golfier S, Herold C, Klaue D, Girardo S, Pagliara S, Ekpenyong A, Jacobi A, *et al.* (2015). Real-time deformability cytometry: on-the-fly cell mechanical phenotyping. Nat Methods 12, 199–202, 4 p following 202.
Paszek MJ, Zahir N, Johnson KR, Lakins JN, Rozenberg GI, Gefen A, Reinhart-King CA, Margulies SS, Dembo M, Boettiger D, *et al.* (2005). Tensional homeostasis and the malignant phenotype. Cancer Cell 8, 241–254.
Pickup MW, Mouw JK, Weaver VM (2014). The extracellular matrix modulates the hallmarks of cancer. EMBO Rep 15, 1243–1253.
Provenzano PP, Inman DR, Eliceiri KW, Beggs HE, Keely PJ (2008a). Mammary epithelial-specific disruption of focal adhesion kinase retards tumor formation and metastasis in a transgenic mouse model of human breast cancer. Am J Pathol 173, 1551–1565.
Provenzano PP, Inman DR, Eliceiri KW, Keely PJ (2009). Matrix density-induced mechanoregulation of breast cell phenotype, signaling and gene expression through a FAK-ERK linkage. Oncogene 28, 4326–4343.
Provenzano PP, Inman DR, Eliceiri KW, Knittel JG, Yan L, Rueden CT, White JG, Keely PJ (2008b). Collagen density promotes mammary tumor initiation and progression. BMC Med 6, 11.
Ricca BL, Venugopalan G, Furuta S, Tanner K, Orellana WA, Reber CD, Brownfield DG, Bissell MJ, Fletcher DA (2018). Transient external force induces phenotypic reversion of malignant epithelial structures via nitric oxide signaling. Elife 7, e26161.
Schedin P, Keely PJ (2011). Mammary gland ECM remodeling, stiffness, and mechanosignaling in normal development and tumor progression. Cold Spring Harb Perspect Biol 3, a003228.
Selhuber-Unkel C, Yde P, Berg-Sørensen K, Oddershede LB (2009). Variety in intracellular diffusion during the cell cycle. Phys Biol 6, 025015.
Solon J, Levental I, Sengupta K, Georges PC, Janmey PA (2007). Fibroblast adaptation and stiffness matching to soft elastic substrates. Biophys J 93, 4453–4461.
Sporn MB (1996). The war on cancer. Lancet 347, 1377–1381.
Swaminathan V, Mythreye K, O'Brien ET, Berchuck A, Blobe GC, Superfine R (2011). Mechanical stiffness grades metastatic potential in patient tumor cells and in cancer cell lines. Cancer Res 71, 5075–5080.
Toepfner N, Herold C, Otto O, Rosendahl P, Jacobi A, Kräter M, Stächele J, Menschner L, Herbig M, Ciuffreda L, *et al.* (2018). Detection of human disease conditions by single-cell morpho-rheological phenotyping of blood. Elife 7.
Tolić-Nørrelykke IM, Munteanu E-L, Thon G, Oddershede L, Berg-Sørensen K (2004). Anomalous diffusion in living yeast cells. Phys Rev Lett 93, 078102.
Ulrich TA, Jain A, Tanner K, MacKay JL, Kumar S (2010). Probing cellular mechanobiology in three-dimensional culture with collagen-agarose matrices. Biomaterials 31, 1875–1884.
Venning FA, Wullkopf L, Erler JT (2015). Targeting ECM disrupts cancer progression. Front Oncol 5, 224.
Wolf K, Mazo I, Leung H, Engelke K, von Andrian UH, Deryugina EI, Strongin AY, Bröcker E-B, Friedl P (2003). Compensation mechanism in tumor cell migration: mesenchymal-amoeboid transition after blocking of pericellular proteolysis. J Cell Biol 160, 267–277.
Yeh W-C, Li P-C, Jeng Y-M, Hsu H-C, Kuo P-L, Li M-L, Yang P-M, Lee P-H (2002). Elastic modulus measurements of human liver and correlation with pathology. Ultrasound Med Biol 28, 467–474.